

Observation of Magnetic Monopoles in Spin Ice

Hiroaki Kadowaki,^{1*} Naohiro Doi,¹ Yuji Aoki,¹ Yoshikazu Tabata,²
Taku J. Sato,³ Jeffrey W. Lynn,⁴ Kazuyuki Matsuhira,⁵ Zenji Hiroi⁶

¹Department of Physics, Tokyo Metropolitan University,
Hachioji-shi, Tokyo 192-0397, Japan.

²Department of Materials Science and Engineering, Kyoto University,
Kyoto 606-8501, Japan.

³NSL, Institute for Solid State Physics, University of Tokyo,
Tokai, Ibaraki 319-1106, Japan.

⁴NIST Center for Neutron Research, National Institute of Standards and Technology,
Gaithersburg, Maryland 20899-6102, USA.

⁵Department of Electronics, Faculty of Engineering, Kyushu Institute of Technology,
Kitakyushu 804-8550, Japan.

⁶Institute for Solid State Physics, University of Tokyo,
Kashiwa 277-8581, Japan.

*To whom correspondence should be addressed. E-mail: kadowaki@phys.metro-u.ac.jp

International Conference on Neutron Scattering 2009 (May 7, 2009; ICNS2009 C9.2)

From the symmetry of Maxwell's equations of electromagnetism as well as field theoretical arguments, magnetic charges or monopoles would be expected to exist. But magnetic monopoles have never been observed despite longstanding experimental searches. Recently, attention has turned to condensed matter systems where tractable analogs of magnetic monopoles might be found, and one prediction is for an emergent elementary excitation in the spin ice compound, where the strongly competing magnetic interactions exhibit the same

type of frustration as water ice. We directly probe the monopoles in spin ice using neutrons, and show that they interact via the magnetic Coulomb force. Specific heat measurements show that the density of monopoles can be controlled by temperature and magnetic field, with the density following the expected Arrhenius law.

From the symmetry of Maxwell's equations of electromagnetism (1), electric charges produce electric fields and magnetic charges or monopoles would produce magnetic fields; moving electric and magnetic charges produce magnetic and electric fields, respectively. At present, magnetic monopoles are absent in the classical equations, because they appear only as pairs of + and - charges, i.e., magnets. About 80 years ago, a quantum mechanical hypothesis of the existence of magnetic monopoles was proposed by Dirac (2). Since then, many experimental searches have been performed, ranging from a monopole search in rocks of the moon to experiments using high energy accelerators (3). But none of them was successful, and the monopole is an open question in experimental physics. Theoretically, monopoles are predicted in grand unified theories, beyond the standard model of particle physics, as topological defects in the energy range of the order 10^{16} GeV (3). However these enormous energies preclude all hope of creating them in any present-day laboratory experiments.

Alternatively, recent theories predict that analogs of the magnetic monopole can be observed in condensed matter systems (4-6). An interesting example (5) is a monopole analog that can be created in the archetypal spin ice compound $\text{Dy}_2\text{Ti}_2\text{O}_7$ (7, 8) with readily accessible energies of the order 10^{-4} eV. In solid water, the protons are disordered even at absolute zero temperature and thus retain finite entropy (9), and spin ice is a magnetic material that exhibits the same type of disordered ground state (8, 10). Here the Dy spins occupy a cubic pyrochlore lattice, which is a corner sharing network of tetrahedra, and the strongly competing magnetic interactions cannot all be satisfied, resulting in a frustrated magnetic ground state (Fig. 1A).

Each spin is parallel to a local [111] easy axis, and interacts with neighboring spins via an effective ferromagnetic coupling. This brings about a geometrical constraint where the lowest energy spin configurations on each tetrahedron follow the ice rule, in which two spins point inward and two point outward on each tetrahedron. This “2-in, 2-out” ground state spin structure has a six-fold degeneracy (Fig. 1A), and the possible ground states of the entire tetrahedral network are macroscopically degenerate in the same way as the disordered protons in water ice (9,10). In addition to this remarkable observation, there is the more intriguing possibility (5) that the excitations from these highly degenerate ground states are topological in nature and mathematically equivalent to magnetic monopoles.

The macroscopic degeneracy of the spin ice state can be simplified by applying a small magnetic field along a [111] direction (11). Along this direction the pyrochlore lattice consists of a stacking of triangular and kagomé lattices (Fig. 1A). In this field-induced ground state, the spins on the triangular lattices are parallel to the field and consequently drop out of the problem, while those on the kagomé lattices retain disorder under the same ice rules, only with a smaller zero-point entropy (12). This is referred to as the kagomé ice state (11, 13–15) (Fig. 1B, inset of Fig. 3), which serves as our vacuum state for the creation of magnetic monopoles.

In Fig. 1C we illustrate creation of a magnetic monopole and antimonopole pair in the vacuum (kagomé ice) state. An excitation is generated from the vacuum by flipping a spin on the kagomé lattice, which results in ice-rule-breaking “3-in, 1-out” (magnetic monopole) and “1-in, 3-out” (anti-monopole) tetrahedral neighbors (Fig. 1C). From the viewpoint of the dumbbell model (5), where a magnetic moment is replaced by a pair of magnetic charges, the ice-rule-breaking tetrahedra simulate magnetic monopoles, with net positive and negative charges sitting on the centers of tetrahedra. The excitation energy for creation of a monopole pair is the order of 10^{-4} eV, corresponding to a thermal energy of 1 K. The monopoles should interact via the magnetic Coulomb force (5), which is brought about by the dipolar interaction (16) between

spins in $\text{Dy}_2\text{Ti}_2\text{O}_7$. They can move and separate by consecutively flipping spins, but are confined to the two-dimensional kagomé layer (e.g. Fig. 1D). This possibility of separating the local excitation into its constituent parts is a novel fractionalization in a frustrated system in two or three dimensions (5, 17), and enables many new aspects of these emergent excitations to be studied experimentally, such as pair creation and interaction, individual motion, currents of monopoles and their concomitant electric field, correlations and cooperative phenomena. In the present study, inspired by the theoretical prediction of the monopoles, we have investigated two aspects of magnetic monopoles in spin ice using direct (microscopic) neutron scattering techniques and thermodynamic (macroscopic) specific heat measurements (18).

A straightforward signature of monopole-pair creation is an Arrhenius law in the temperature (T) dependence of the specific heat (C), $C(T) \propto \exp(-\Delta E/k_{\text{B}}T)$, where ΔE is a field (H) dependent creation energy. One can simply expect $\Delta E = E_0 - \mu H$ owing to the Zeeman effect. Figure 2A shows the measured $C(T)$ of $\text{Dy}_2\text{Ti}_2\text{O}_7$ under a [111] applied field as a function of $1/T$ (18). The Arrhenius law is clearly seen at low temperatures, indicating that monopole–antimonopole pairs are thermally activated from the ground state ‘vacuum’. The observed activation energy ΔE depends linearly on H (Fig. 2B) between 0.2 and 0.9 T, i.e., in the kagomé ice state (inset of Fig. 3). The zero-field value $\Delta E(H = 0) = 3.5$ K reasonably agrees with an estimation $\Delta E(H = 0) = 4J_{\text{eff}} = 4.5$ K using the nearest-neighbor effective bond energy J_{eff} (16). The observed Arrhenius law of $C(T)$, which is attributable to variation of density of the monopole pairs, implies that the number of monopoles can be tuned by changing T and H .

A microscopic experimental method of observing monopoles is to perform magnetic neutron scattering using the neutron’s dipole moment as the probe. One challenge to the experiments is to distinguish the relatively weak scattering from the small number of monopoles from the very strong magnetic scattering (8, 14) of the ground state ‘vacuum’. A theoretical idea (5)

which is helpful for identifying the monopole scattering is that the [111] field acts as chemical potential of the monopoles, enabling us to control their density as shown by the present specific heat measurements. As the field is increased, the kagomé ice state with low monopole density (Fig. 1B) changes continuously to the maximum density state, the staggered monopole state (Fig. 1E), where all spin configurations become “3-in, 1-out” or “1-in, 3-out” to minimize the Zeeman energy.

For the present neutron scattering experiments, the best temperature and field region to observe monopoles in $\text{Dy}_2\text{Ti}_2\text{O}_7$ is close to the liquid-gas type critical point ($I3$) (T_c, H_c) (inset of Fig. 3). In the monopole picture (5), where they are interacting via the magnetic Coulomb force, the first-order phase transition ($I3$) is ascribed to phase separation between high- and low-density states. We naturally anticipate that neutron scattering close to the critical point is a superposition of the scattering pattern by the (low-density) kagomé ice state ($I4$) and that by high-density monopoles, which is diffuse scattering around magnetic Bragg reflections, i.e., ferromagnetic fluctuations. It should be noted that the superposed scattering patterns would provide strong evidence that the magnetic Coulomb force really acts between monopoles.

The neutron measurements were performed under a [111] applied magnetic field ($I8$), and Monte Carlo (MC) simulations were also carried out for the dipolar spin ice model ($I6, I8, I9$) to quantify our observations. Figure 3 shows the field dependence of the magnetic intensity of the (2,-2,0) Bragg reflection at $T = T_c + 0.05 = 0.43$ K. The intensity plateau for $H < 0.8$ T corresponds to the kagomé ice state with low density monopoles (Fig. 1B). The deviation from the plateau as H exceeds 0.8 T indicates that monopoles are being created gradually (Figs. 1C and 1D), while the saturation of the intensity for $H \gg H_c$ denotes the staggered monopole state (Fig. 1E). In Fig. 3 we also show the Bragg intensity and the density of the positively charged monopoles obtained by the MC simulation, where we slightly shifted the simulated T and H values because the simulated T_c and H_c deviated from the observed values by 0.02 K and 0.05

T, respectively. The observation shows good agreement with the simulation for $H < H_c$. On the other hand, above H_c there are substantially less monopoles than expected from the simulation, which will be discussed below.

We selected $T = T_c + 0.05$ K and $H = H_c$ (inset of Fig. 3) for observation of the fluctuating high- and low-density monopoles. At this H, T point, we measured intensity maps in the scattering plane perpendicular to the [111] field. An intensity map of the kagomé ice state at $T = T_c + 0.05$ K and $H = 0.5$ T (inset of Fig. 3) was also measured for comparison. Figure 4 compares the measured and simulated intensity maps. The observed scattering pattern of the kagomé ice state (Fig. 4A) is in excellent agreement with the simulation (Fig. 4C), showing the peaked structure (14) at $(2/3, -2/3, 0)$ and the pinch point (20) at $(4/3, -2/3, -2/3)$. These structures reflect the vacuum (kagomé ice) state.

The observed (Fig. 4B) and simulated (Fig. 4D) intensity maps close to the critical point show a weakened kagomé-ice scattering pattern (by the low-density state) and diffuse scattering around $(2, -2, 0)$ (by the high-density state). Although the observation agrees fairly well with the simulation, the diffuse scattering is less pronounced for the observation. We found that this discrepancy originated from an instrumental condition of the GPTAS spectrometer (18), which has a large vertical resolution of $\Delta q = 0.25 \text{ \AA}^{-1}$ (full width at half maximum, FWHM). We carried out the same measurement on the BT-9 spectrometer (18), which has a smaller vertical resolution of $\Delta q = 0.1 \text{ \AA}^{-1}$ (FWHM), and which does not affect the diffuse scattering. The resulting data are shown in Fig. 4F, which are in better agreement with the simulation (Fig. 4D) especially around $(2, -2, 0)$. An interesting experimental fact revealed by this resolution effect is that correlations of the high-density monopoles are three dimensional in space, although the monopoles can only move in the two dimensional layers (Fig. 1D). The three dimensional correlations are consistent with the isotropic Coulomb interaction between monopoles. We note that the kagomé-ice scattering pattern is two dimensional in nature (14), and thus is not affected

by the vertical resolution.

To illustrate the high- and low-density monopoles yielding the scattering patterns in Figs. 4B, D and F, two typical snapshots of the monopoles of the MC simulation are shown in Fig. 4E, where we depict magnetic charges at centers of the tetrahedra. Lines connecting the centers of tetrahedra form a diamond lattice, and magnetic charges reside on its lattice points. Regions of the low-density monopoles (where black points dominate) produce the kagomé-ice scattering pattern, while those of the high-density monopoles (where red and blue points dominate) produce the diffuse scattering around the Bragg reflections. These critical fluctuations between high- and low-density phases reinforce the proposed explanation (5) of the puzzling liquid-gas type critical point (13) using the similarity to phase transitions of ionic particle systems on lattices (21). Consequently they provide microscopic evidence of magnetic monopoles and the mutual Coulomb force. Further investigations of critical phenomena, universality class (15), screening of the Coulomb interaction, effects of the anisotropic motion of the monopoles within the kagomé lattices are of interest.

An important question, which is not pursued in the present study, is how monopoles unbound by the fractionalization mechanism move in the kagomé lattice. There may be an interesting hint in the discrepancy between observed magnetic Bragg intensity and the classical MC simulation of Ising spins shown in Fig. 3 ($H > H_c$). It may indicate the existence of quantum mechanical effects neglected in the computation. Similar puzzling experimental facts were also noticed by the slow saturation of magnetization (13) and the non-zero specific heat (15) above H_c down to very low temperatures, $T < 0.1$ K, suggesting quantum effects. For example, if the double spin flips shown in Fig. 1D can occur by quantum tunneling (22), monopoles (or holes in the staggered monopole state) might move more easily than classical diffusion (23) at low temperatures, possibly giving rise to soft modes. Comparing the Arrhenius law with that of a recent theoretical study (23) of the diffusive motion of monopoles in spin ice state ($H = 0$), it seems

that the interesting high temperature ranges where unconfined monopoles move diffusively are roughly $T > 1.5$ K ($H = 0.5$ T) and $T > 0.7$ K ($H = 0.9$ T).

Typical elementary excitations in condensed matter, such as acoustic phonons and (gapless) magnons, are Nambu-Goldstone modes where a continuous symmetry is spontaneously broken when the ordered state is formed. This contrasts with the monopoles in spin ice, which are point defects that can be fractionalized in the frustrated ground states. Such excitations are unprecedented in condensed matter, and will now enable conceptually new emergent phenomena to be explored experimentally.

References and Notes

1. J. D. Jackson, *Classical Electrodynamics* (Wiley, New York, 1975) chap. 6.12-6.13.
2. P. A. M. Dirac, *Proc. R. Soc. A* **133**, 60 (1931).
3. K. A. Milton, *Rep. Prog. Phys.* **69**, 1637 (2006).
4. Z. Fang *et al.*, *Science* **302**, 92 (2003).
5. C. Castelnovo, R. Moessner, S. L. Sondhi, *Nature* **451**, 42 (2008).
6. X-L. Qi, R. Li, J. Zang, S-C. Zhang, *Science* **323**, 1184 (2009).
7. M. J. Harris, S. T. Bramwell, D. F. McMorrow, T. Zeiske, K. W. Godfrey, *Phys. Rev. Lett.* **79**, 2554 (1997).
8. S. T. Bramwell, M. J. P. Gingras, *Science* **294**, 1495 (2001).
9. L. Pauling, *J. Am. Chem. Soc.* **57**, 2680 (1935).
10. A. P. Ramirez, A. Hayashi, R. J. Cava, R. Siddharthan, B. S. Shastry, *Nature* **399**, 333 (1999).

11. K. Matsuhira, Z. Hiroi, T. Tayama, S. Takagi, S. Sakakibara, *J. Phys. Condens. Matter* **14**, L559 (2002).
12. R. Moessner, S. L. Sondhi, *Phys. Rev. B* **68**, 064411 (2003).
13. T. Sakakibara, T. Tayama, Z. Hiroi, K. Matsuhira, S. Takagi, *Phys. Rev. Lett.* **90**, 207205 (2003).
14. Y. Tabata *et al.* *Phys. Rev. Lett.* **97**, 257205 (2006).
15. R. Higashinaka, H. Fukazawa, K. Deguchi, Y. Maeno, *J. Phys. Soc. Jpn.* **73**, 2845 (2004).
16. B. C. den Hertog, M. J. P. Gingras, *Phys. Rev. Lett.* **84**, 3430 (2000).
17. P. Fulde, K. Penc, N. Shannon, *Ann. Phys.* **11**, 892 (2002).
18. Materials and methods are available as supporting material on Science Online.
19. R. G. Melko, M. J. P. Gingras, *J. Phys. Condens. Matter* **16**, R1277 (2004).
20. T. Fennell, S. T. Bramwell, D. F. McMorrow, P. Manuel, A. R. Wildes, *Nature Physics* **3**, 566 (2007).
21. V. Kobelev, A. B. Kolomeisky, M. E. Fisher, *J. Chem. Phys.* **116**, 7589 (2002).
22. G. Ehlers *et al.*, *J. Phys. Condens. Matter* **15**, L9 (2003).
23. L. D. C. Jaubert, P. C. W. Holdsworth, *Nature Physics* **5**, 258 (2009).
24. We thank R. Higashinaka and Y. Maniwa for discussions. The present work is supported by KAKENHI and the US-Japan Cooperative Program on Neutron Scattering, Neutron Science Laboratory, Materials Design and Characterization Laboratory and Supercomputer Center of Institute for Solid State Physics, University of Tokyo.

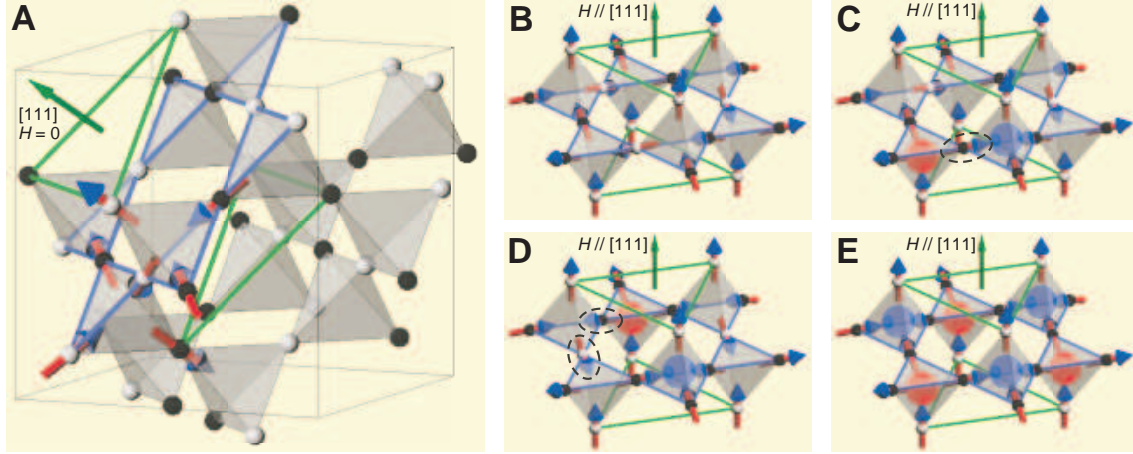


Figure 1: Magnetic moments of $\text{Dy}_2\text{Ti}_2\text{O}_7$ reside on the corners of tetrahedra of the cubic pyrochlore lattice (8). They are represented by arrows pointing inward or outward from centers of the tetrahedra. At low temperatures, four magnetic moments on each tetrahedron obey the ice rule (2-in, 2-out) to minimize the effective ferromagnetic interaction. The resulting spin ice state consists of a macroscopic number of disordered configurations, an example of which is shown in (A). The pyrochlore lattice consists of stacked triangular and kagomé lattices, shown by green and blue lines, respectively, along a $[111]$ direction. (B) Under small $[111]$ magnetic fields, spins on the triangular lattices become parallel to the field and drop out of the problem, while the spins on the kagomé lattice remain in the disordered kagomé ice state (11). (C) An excited state is induced by flipping a spin from (B), enclosed by a dashed circle, where neighboring tetrahedra have 3-in, 1-out and 1-in, 3-out configurations. These ice-rule-breaking tetrahedra are represented by magnetic monopoles with opposite charges depicted by blue and red spheres. (D) By consecutively flipping two spins from (C), the monopoles are fractionalized. (E) As the magnetic field is increased, $H \gg H_c$, spins realize a fully ordered, staggered arrangement of monopoles.

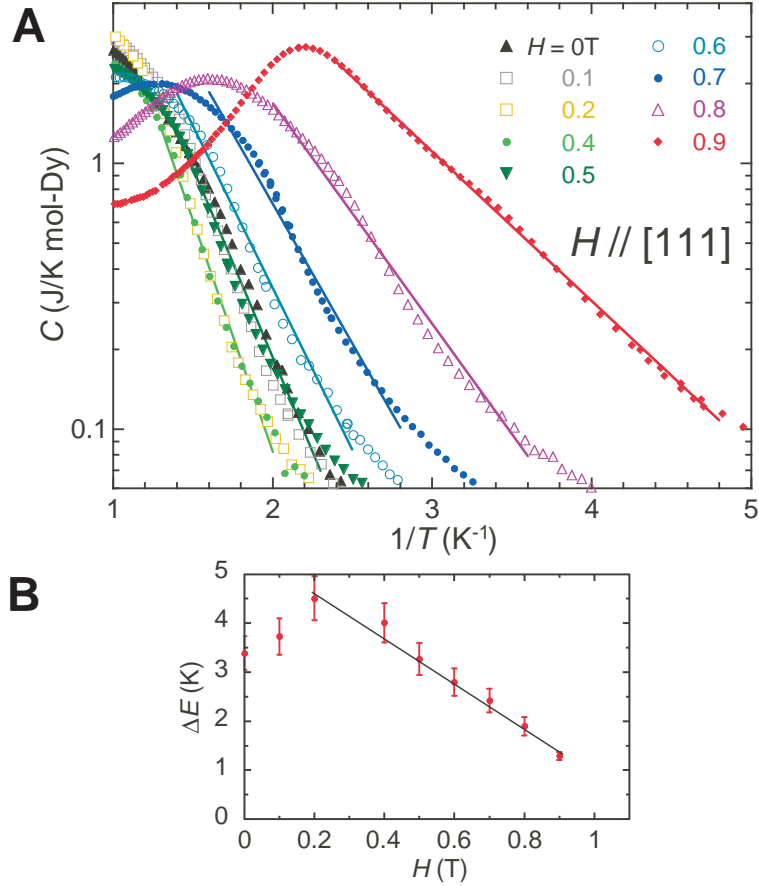


Figure 2: **(A)** Specific heat of $\text{Dy}_2\text{Ti}_2\text{O}_7$ under an applied magnetic field in the $[111]$ direction is plotted as a function of $1/T$. In the intermediate temperature range these data are well represented by the Arrhenius law denoted by solid lines. **(B)** Field dependence of the activation energy ΔE . The solid line represents a linear function of H with the slope expected by the Zeeman effect. The deviation from linearity below 0.2 T (spin ice regime) suggests that J_{eff} slightly changes between the spin and kagomé ice states. We remark that all the measurements were performed under field cooling conditions, which are important to avoid complications due to spin freezing (8, 10, 19) among the ground state manifolds.

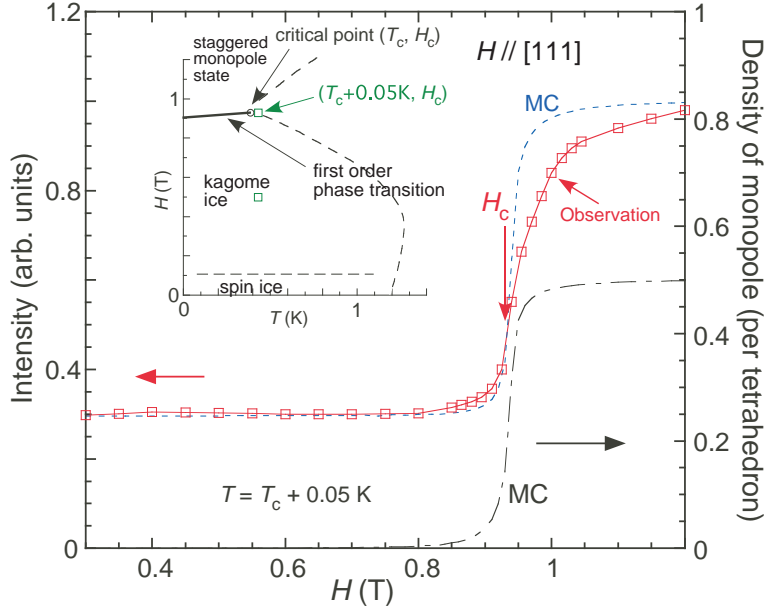


Figure 3: The magnetic Bragg intensity at $T = T_c + 0.05$ K is plotted as a function of the [111] magnetic field strength. The open squares and dashed curves represent the neutron scattering measurements at (2,-2,0) and corresponding MC simulations, respectively. The dot-dashed curve is the density of positively charged monopoles obtained by the MC simulation (18). (Inset) The HT phase diagram under the [111] magnetic field. The solid line represents the first-order phase transition with the critical point shown by an open circle (13). The dashed lines are crossovers (15). The intensity maps shown in Fig. 4 were measured at the two points depicted by open squares.

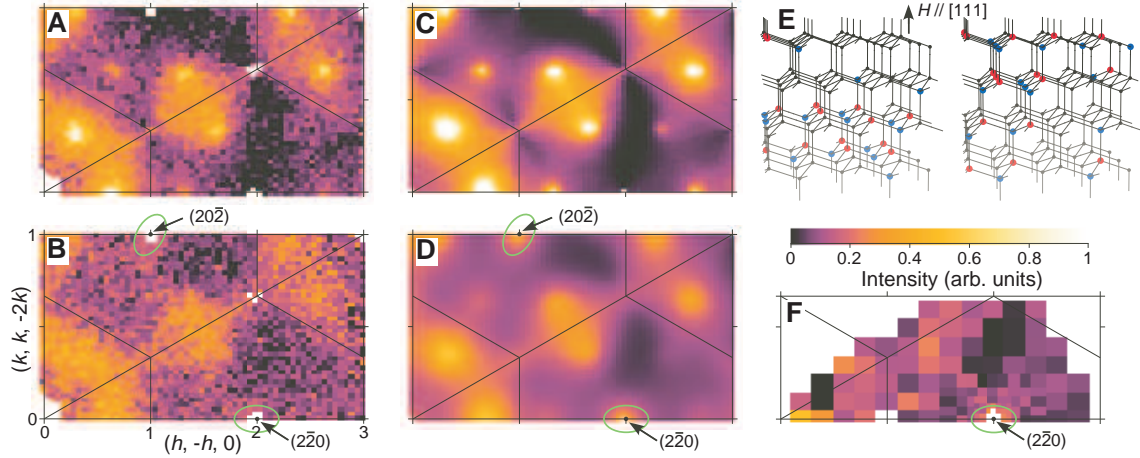


Figure 4: Intensity maps of neutron scattering measured at $T = T_c + 0.05$ K in the scattering plane perpendicular to the $[111]$ field are shown for two field-temperature values shown by open squares in the inset of Fig. 3: the kagomé ice state at $H = 0.5$ T (**A,C**) and the fluctuating high- and low-density monopoles at $H = H_c$ (**B,D,F**). (**A,B**) and (**F**) were measured on the GPTAS and BT-9 spectrometers, respectively (18). To clearly show the six-fold symmetry, the drawing range of (**A,B**) is extended from the measured range $k < (h + 0.2)/3$ using the crystal symmetry. (**C,D**) are calculated intensities using the MC simulations (18). (**E**) two snapshots of the monopoles of the MC simulation corresponding to (**B,D,F**) are shown on the diamond lattice connecting the centers of the tetrahedra, in which blue, red and black points represents $+$, $-$ and 0 magnetic charges, respectively. The light green circles enclosing $(2,-2,0)$ and $(2,0,-2)$ in (**B,D,F**) show the high intensity regions caused by the high-density monopoles, i.e., ferromagnetic fluctuations.

Supporting online material

Materials and Methods

Single crystals of $\text{Dy}_2\text{Ti}_2\text{O}_7$ were prepared by the floating-zone method (1, 2) using an infrared furnace equipped with four halogen lamps and elliptical mirrors. The crystals were grown under O_2 gas flow to avoid oxygen deficiency with a growth rate of 4 mm/h. Single crystal samples used in the neutron scattering and specific heat experiments were $22 \times 3.1 \times 0.58 \text{ mm}^3$ and $8.7 \times 1.0 \times 0.28 \text{ mm}^3$, respectively, in size. Their long directions are parallel to [111] directions within 1.5 degrees, which ensures negligibly small demagnetization effect.

Neutron scattering experiments on the single crystal under a [111] applied magnetic field were performed on the triple-axis spectrometers BT-9 at the NIST Center for Neutron Research and the ISSP-GPTAS at the Japan Atomic Energy Agency. They are equipped with PG(002) monochromator and analyzer. We operated them using an initial energy of $E_i = 30.5 \text{ meV}$, with the analyzer angle fixed at the elastic position, and removed higher order neutrons by PG filters. The sample was mounted in dilution refrigerators so as to measure the scattering plane perpendicular to the [111] direction. All the data shown are corrected for background and absorption.

Specific heat of the single crystalline sample was measured down to 0.1 K by a quasi-adiabatic heat-pulse method using a dilution refrigerator equipped with an 8-T superconducting magnet. The sample was mounted on the addenda (made of a copper plate) of the specific-heat measurement-cell so that the magnetic field was applied along a [111] direction. A field-calibrated RuO_2 thermometer on the addenda was used to measure the sample temperature. The temperature increment caused by each heat pulse was controlled to be $\Delta T/T = 0.5 \sim 1 \%$ by a computer. In order to avoid complications due to possible spin freezing among the ground state manifolds, all the measurements were performed after field cooling from temperatures above

2 K. The resulting data are in reasonable agreement with the previous reports (1–3). At low temperatures, more accurate measurements were carried out using long time T -response measurement with longer heat pulses (~ 50 sec) and a data fitting procedure which fully deals with the so called “tau-2” effect brought about by the existence of slow thermal response components in the sample. The accuracy of these measurements was confirmed through nuclear specific heat studies using the same measurement system (4, 5).

The MC simulations of the dipolar spin ice $\text{Dy}_2\text{Ti}_2\text{O}_7$ (6) were carried out partly by using a supercomputer at Institute for Solid State Physics, University of Tokyo. We adopted the Hamiltonian describing the Ising spin system as follows (7):

$$\mathcal{H} = -\mu_{\text{eff}} \sum_{i,a} \mathbf{S}_i^a \cdot \mathbf{H} - \sum_{\langle(i,a),(j,b)\rangle} J_{i,a;j,b} \mathbf{S}_i^a \cdot \mathbf{S}_j^b + D r_{\text{nn}}^3 \sum \left[\frac{\mathbf{S}_i^a \cdot \mathbf{S}_j^b}{|\mathbf{R}_{ij}^{ab}|^3} - \frac{3(\mathbf{S}_i^a \cdot \mathbf{R}_{ij}^{ab})(\mathbf{S}_j^b \cdot \mathbf{R}_{ij}^{ab})}{|\mathbf{R}_{ij}^{ab}|^5} \right],$$

where \mathbf{S}_i^a represents the spin vector parallel to the local $\langle 111 \rangle$ easy axis, with $|\mathbf{S}_i^a| = 1$ at the sublattice site a in the unit cell of the fcc lattice site i . The first term is the Zeeman interaction between the spins possessing the effective moment $\mu_{\text{eff}} \simeq 10 \mu_{\text{B}}$ and the magnetic field \mathbf{H} . The second and third terms are the exchange and dipolar interactions, respectively. We used the same parameters of the dipolar interaction and the exchange couplings as reported in (8): $D = 1.41$ K, $J_1 = -3.72$ K, $J_2 = 0.1$ K and $J_3 = -0.03$ K. A standard Metropolis algorithm with single-spin-flip dynamics was used in the MC simulations (6). We simulated up to $21 \times 21 \times 7$ hexagonal cells (37044 spins), and averaged data of magnetic scattering intensities over up to $\sim 2 \times 10^6$ MC steps per spin.

1. K. Matsuhira, Z. Hiroi, T. Tayama, S. Takagi, S. Sakakibara, *J. Phys. Condens. Matter* **14**, L559 (2002).
2. Z. Hiroi, K. Matsuhira, S. Takagi, T. Tayama, T. Sakakibara, *J. Phys. Soc. Jpn.* **72**, 411

(2003).

3. R. Higashinaka, H. Fukazawa, K. Deguchi, Y. Maeno, *J. Phys. Soc. Jpn.* **73**, 2845 (2004).
4. Y. Aoki *et al.*, *Phys. Rev. B* **65**, 064446 (2002).
5. Y. Aoki *et al.*, *J. Phys. Soc. Jpn.* **71**, 2098 (2002).
6. R. G. Melko, M. J. P. Gingras, *J. Phys. Condens. Matter* **16**, R1277 (2004).
7. J. P. C. Ruff, R. G. Melko, M. J. P. Gingras, *Phys. Rev. Lett.* **95**, 097202 (2005).
8. Y. Tabata *et al.* *Phys. Rev. Lett.* **97**, 257205 (2006).